Adjoint Methods in a Higher-Order Space-Time Discontinuous-Galerkin Solver for Turbulent Flows

Laslo Diosady
Science & Technology Corp.

Patrick Blonigan
USRA

Scott Murman
NASA ARC

Anirban Garai
Science & Technology Corp.

Motivation

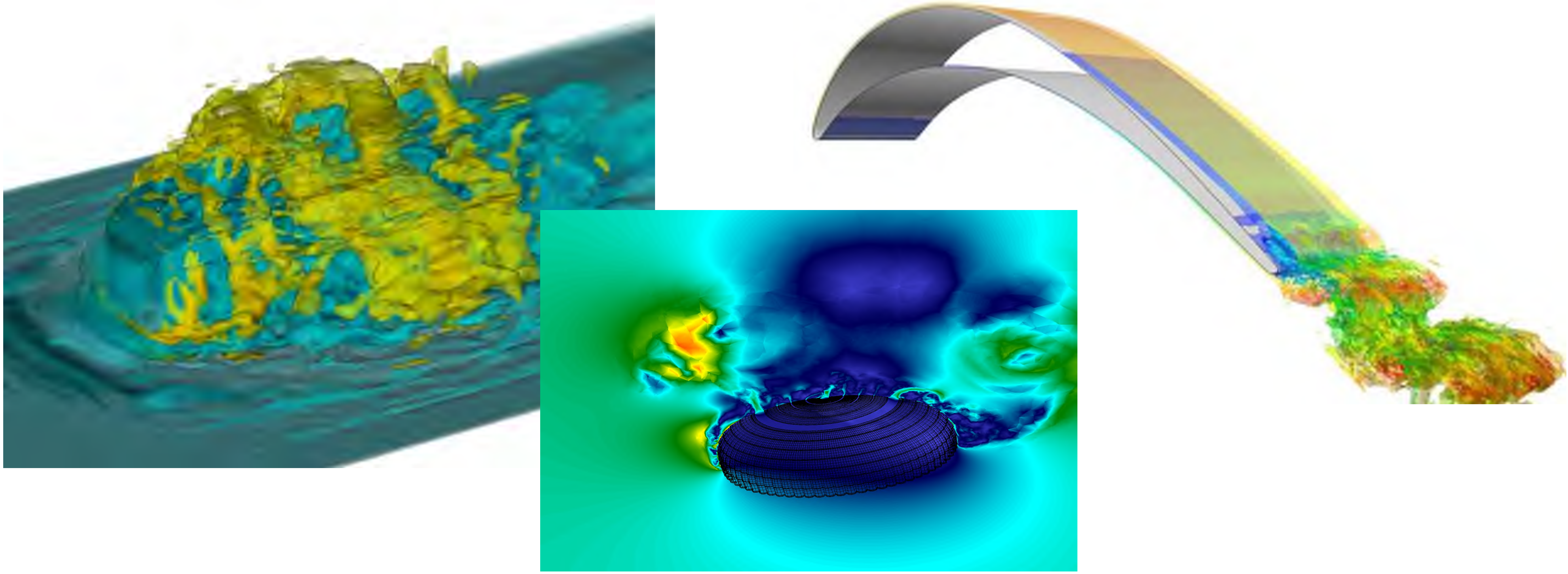

- Perform detailed time-accurate scale-resolving simulations of practical, complex, compressible flows
- High-Reynolds-number separated flows involving large-scale unsteadiness, where RANS models are unreliable

Approach

- Turbulent flows involve a large range of spatial and temporal scales which need to be resolved
- Efficient algorithms and implementation necessary for wall-resolved high Reynolds number flows
- Numerical method must be capable of handling complex geometry
- Numerical method must be “robust”

Developed higher-order space-time discontinuous-Galerkin spectral element framework

Approach

- Gradient computation needed for error-estimation, adaptation, design, sensitivity analysis, etc.
- Tangent and adjoint methods have been successfully applied to a variety of steady and unsteady flows
- High-fidelity simulations we are targeting are chaotic
- Can traditional tangent/adjoint methods work?
- **Develop efficient implementation of tangent and adjoint method in space-time discontinuous solver**
- **Assess the applicability of traditional adjoint and tangent methods for chaotic flows**

Outline

- Space-time DG formulation
  - Discrete primal formulation
  - Discrete tangent and adjoint formulations
- NACA0012
  - Flow sensitivity with increasing Reynolds number
  - Properties of adjoint for chaotic flows
- T106a LPT
  - Adjoint solutions corresponding to a practical simulation
- Summary/Outlook

Space-Time Discontinuous-Galerkin (DG) Formulation

- Compressible Navier-Stokes Equations: $$\frac{\partial u}{\partial t} + \nabla \cdot F(u, \nabla u) = 0$$
- Space-Time Discontinuous-Galerkin Discretization:
  - Entropy variables: Hughes (1986)

$$\underbrace{A_o}_{\text{SPD}} v_{,t} + \underbrace{A_i}_{\text{Sym}} v_{,i} - (\underbrace{K_{ij}}_{\text{SPSD}} v_{,j})_{,i} = 0$$

$$v = \begin{bmatrix} -\frac{s}{\gamma-1} + \frac{\gamma+1}{\gamma-1} - \frac{\rho E}{p} \\ \frac{\rho u_i}{p} \\ -\frac{\rho}{p} \end{bmatrix}$$

  - Inviscid Flux: Ismail & Roe (2009)
  - Viscous Flux: Interior penalty method with penalty parameter given by 2nd method of Bassi and Rebay (2007)
  - Integrals evaluated using numerical quadrature with 2N points
  - Discrete entropy stability: Barth (1995)

$$(\rho s)_{,t} + \left(\frac{q_i}{c_v T}\right)_{,i} = v_{,i}^T K_{ij} v_{,j} \geq 0$$

Discrete Formulation

- Discrete system solved each time-slab:

$$R^n(u^n, w^n) + G^n(u^{n-1}, w^n) = 0$$

  - where:

$$R^n(u^n, w^n) = \sum_{\kappa} \left\{ \int_I \int_{\kappa} - \left(\frac{\partial w}{\partial t} u + \nabla w \cdot F \right) + \int_I \int_{\partial \kappa} w \widehat{F \cdot n} + \int_{\kappa} w(t_-^{n+1}) u(t_-^{n+1}) \right\}$$

$$G^n(u^{n-1}, w^n) = \sum_{\kappa} \left\{ \int_{\kappa} -w(t_+^n) u(t_-^n) \right\}$$

    - beginning/end of time-slab

$$w(t_+^n) = I_s w^n \qquad w(t_-^{n+1}) = I_e w^n$$

Discrete Tangent formulation

- Output: $J(u;\alpha)$
  - where α is a parameter (i.e. angle of attack, Reynolds number etc.)
- Compute sensitivity of output to parameters:

$$\frac{dJ}{d\alpha} = \frac{\partial J}{\partial \alpha} + \frac{\partial J}{\partial u}\frac{\partial u}{\partial \alpha} = \frac{\partial J}{\partial \alpha} + \frac{\partial J}{\partial \bar{R}}\frac{\partial \bar{R}}{\partial \alpha}$$

- Tangent equation:

$$\frac{\partial R^n}{\partial u^n}(\delta u^n, w^n) + \frac{\partial G^n}{\partial u^{n-1}}(\delta u^{n-1}, w^n) = -\frac{\partial R^n}{\partial \alpha}$$

- Matrix form:

$$\begin{bmatrix} \frac{\partial R^{n-1}}{\partial u^{n-1}} & 0 & 0 \\ \frac{\partial G^n}{\partial u^{n-1}} & \frac{\partial R^n}{\partial u^n} & 0 \\ 0 & \frac{\partial G^{n+1}}{\partial u^n} & \frac{\partial R^{n+1}}{\partial u^{n+1}} \end{bmatrix} \begin{bmatrix} \delta u^{n-1} \\ \delta u^n \\ \delta u^{n+1} \end{bmatrix} = -\begin{bmatrix} \frac{\partial R^{n-1}}{\partial u^{n-1}} \\ \frac{\partial R^n}{\partial u^n} \\ \frac{\partial R^{n+1}}{\partial u^{n+1}} \end{bmatrix}$$

Discrete Adjoint Formulation

- Lagrangian: $$\mathcal{L}(u,\psi;\alpha) = J(u;\alpha) + \psi^T \bar{R}(u;\alpha)$$
- Stationarity of Lagrangian:

$$\delta\mathcal{L} = \underbrace{\left(\left.\frac{\partial J}{\partial u}^T\right|_\alpha + \psi^T \left.\frac{\partial \bar{R}}{\partial u}\right|_\alpha \right)}_{\text{Adjoint}} \delta u + \underbrace{\left(\left.\frac{\partial J}{\partial \alpha}^T\right|_u + \psi^T \left.\frac{\partial \bar{R}}{\partial \alpha}\right|_u \right)}_{\text{Sensitivity}} \delta\alpha = 0$$

- Adjoint equation:

$$\frac{\partial R^n}{\partial u^n}(w^n,\psi^n) + \frac{\partial G^n}{\partial u^{n-1}}(w^{n-1},\psi^n) = -\frac{\partial J^n}{\partial u^n}(\psi^n)$$

- Matrix Form:

$$\begin{bmatrix} \frac{\partial R^{n-1}}{\partial u^{n-1}}^T & \frac{\partial G^n}{\partial u^{n-1}}^T & 0 \\ 0 & \frac{\partial R^n}{\partial u^n}^T & \frac{\partial G^{n+1}}{\partial u^n}^T \\ 0 & 0 & \frac{\partial R^{n+1}}{\partial u^{n+1}}^T \end{bmatrix} \begin{bmatrix} \psi^{n-1} \\ \psi^n \\ \psi^{n+1} \end{bmatrix} = -\begin{bmatrix} \frac{\partial J^{n-1}}{\partial u^{n-1}} \\ \frac{\partial J^n}{\partial u^n} \\ \frac{\partial J^{n+1}}{\partial u^{n+1}} \end{bmatrix}$$

Primal Solver: Implementation Details

- **Efficient implementation of higher order DG**
  - Tensor-product basis
  - Take advantage of hardware (SIMD/optimized kernels)
  - Jacobian-free Approximate Newton-Krylov solver
  - Tensor-product based ADI-preconditioner
- Primal Residual Evaluation:
  1. Evaluate state/gradient at quadrature points
  2. Evaluate flux at quadrature points
  3. Weight fluxes with gradient of test functions

Optimized sum-factorization

Vectorized Kernels

Tangent/Adjoint: Implementation Details

- **Reuse optimization from primal for tangent and adjoint**
  - Tangent Residual Evaluation:
    1. Evaluate state/gradient and update/gradient at quadrature points
    2. Evaluate linearized flux at quadrature points
    3. Weight fluxes with gradient of test functions
  - Adjoint Residual Evaluation:
    4. Evaluate state/gradient and adjoint/gradient at quadrature points
    5. Evaluate adjoint flux at quadrature points
    6. Weight fluxes with gradient of test functions

Optimized sum-factorization

Vectorized Kernels

NACA0012, $\alpha = 10$

- At high angle of attack, flow over NACA0012 airfoil exhibits vortex shedding which become chaotic with increasing Reynolds number. (Pulliam 1993)
- Examine primal and adjoint solutions

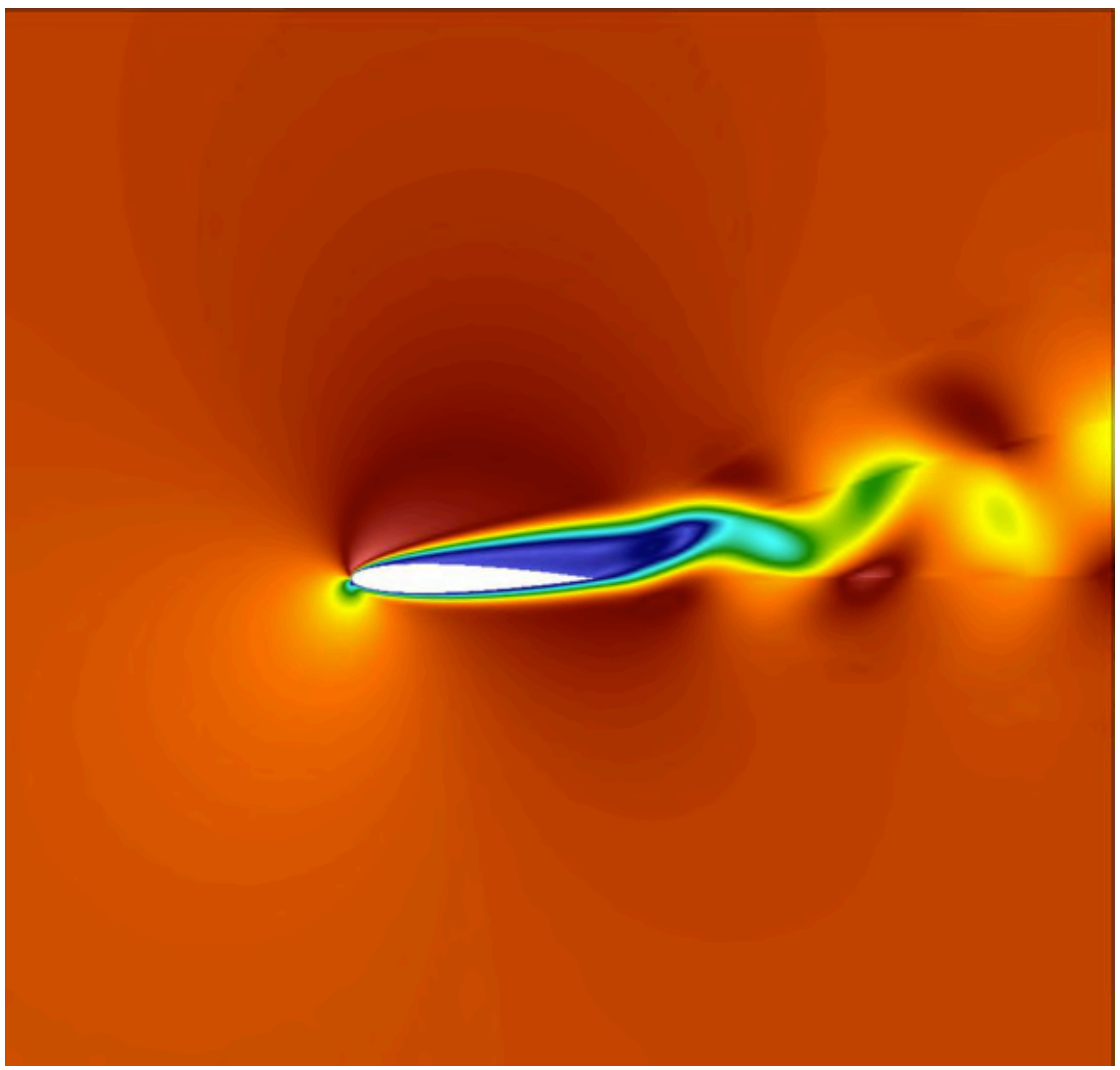

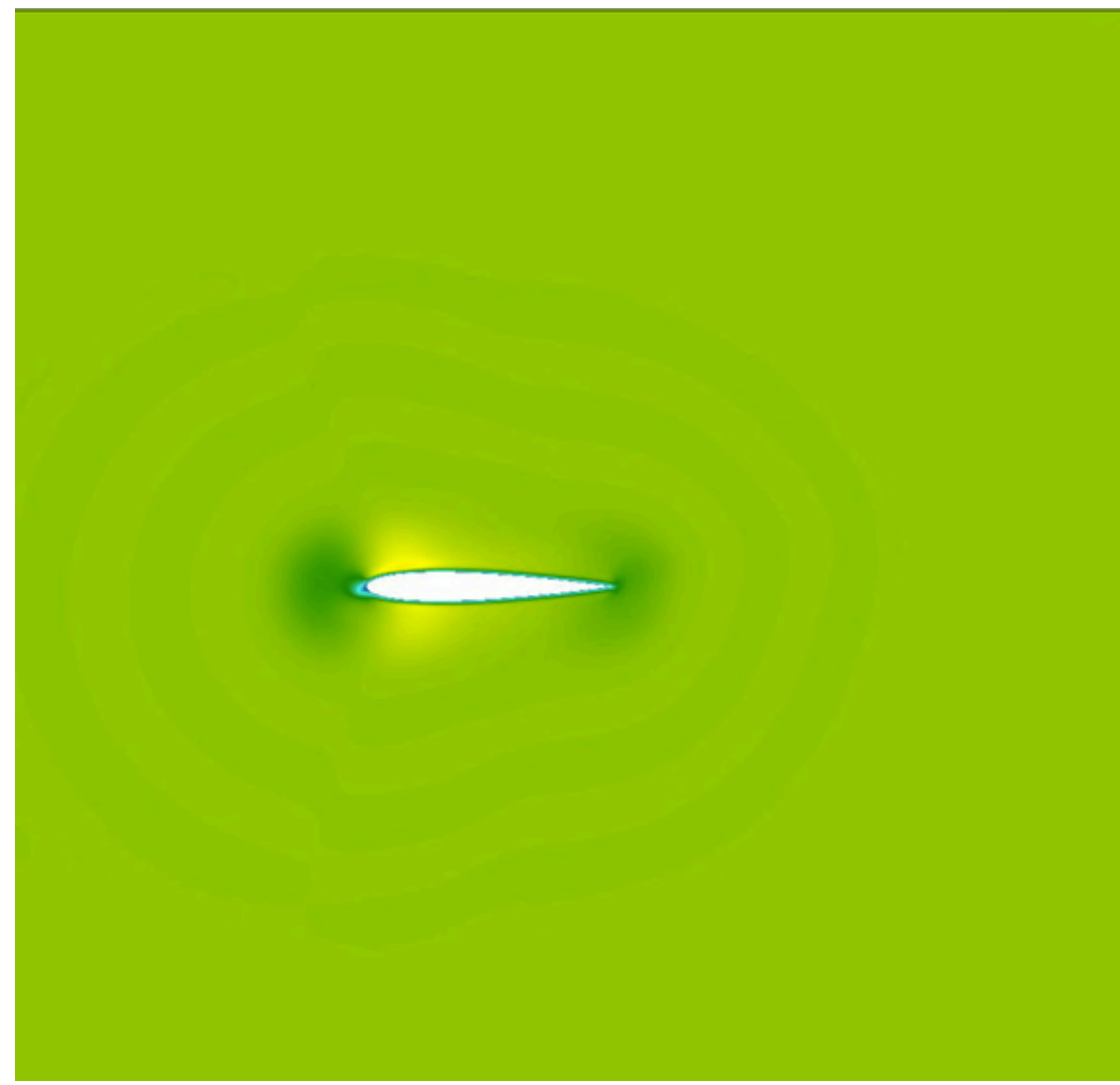

NACA0012, Re = 800, α = 10

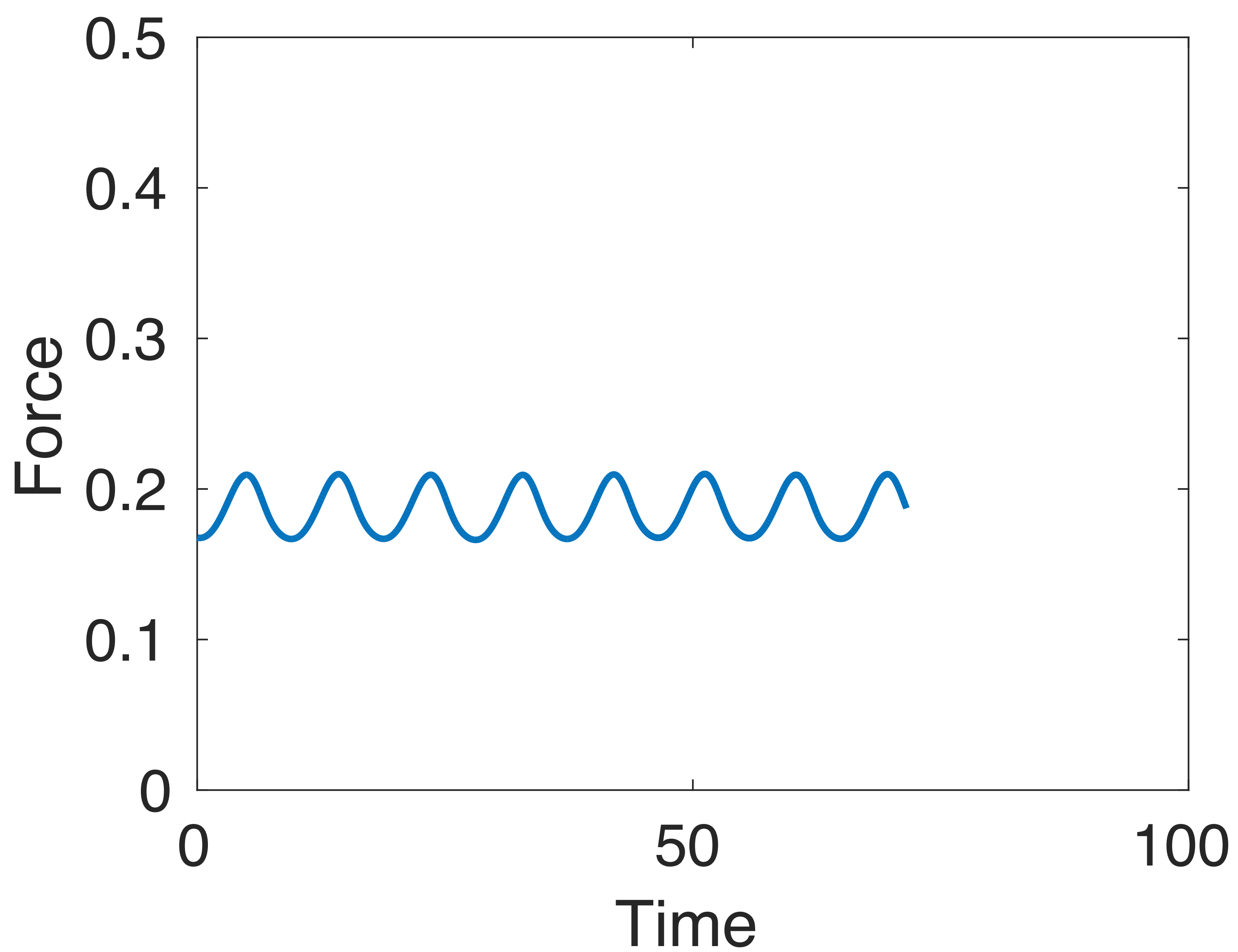

Directional Force Output

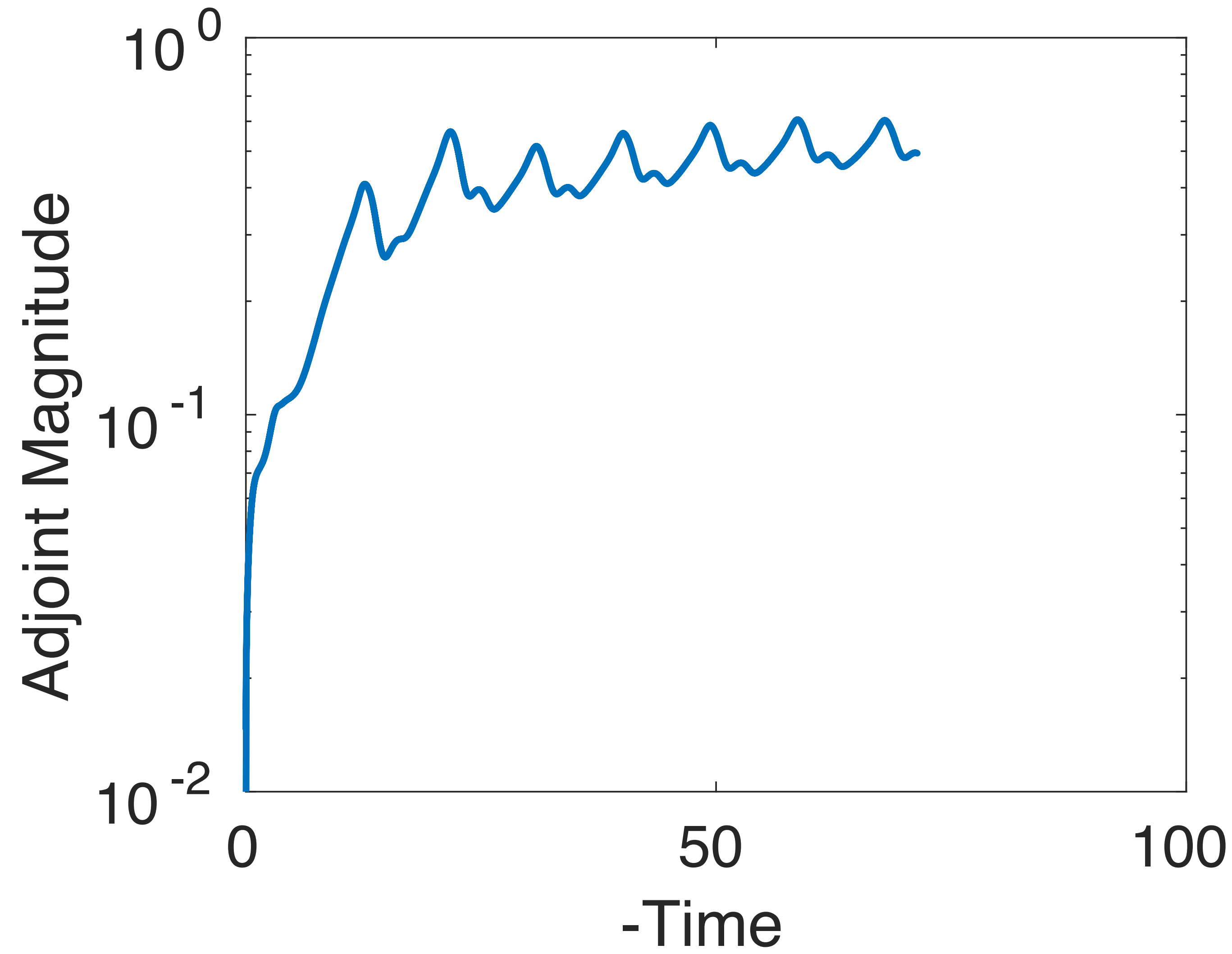

Adjoint Magnitude

- Unsteady shedding gives periodic output signal
- Adjoint solution also periodic (after initial transient)

NACA0012, Re = 1600, α = 10

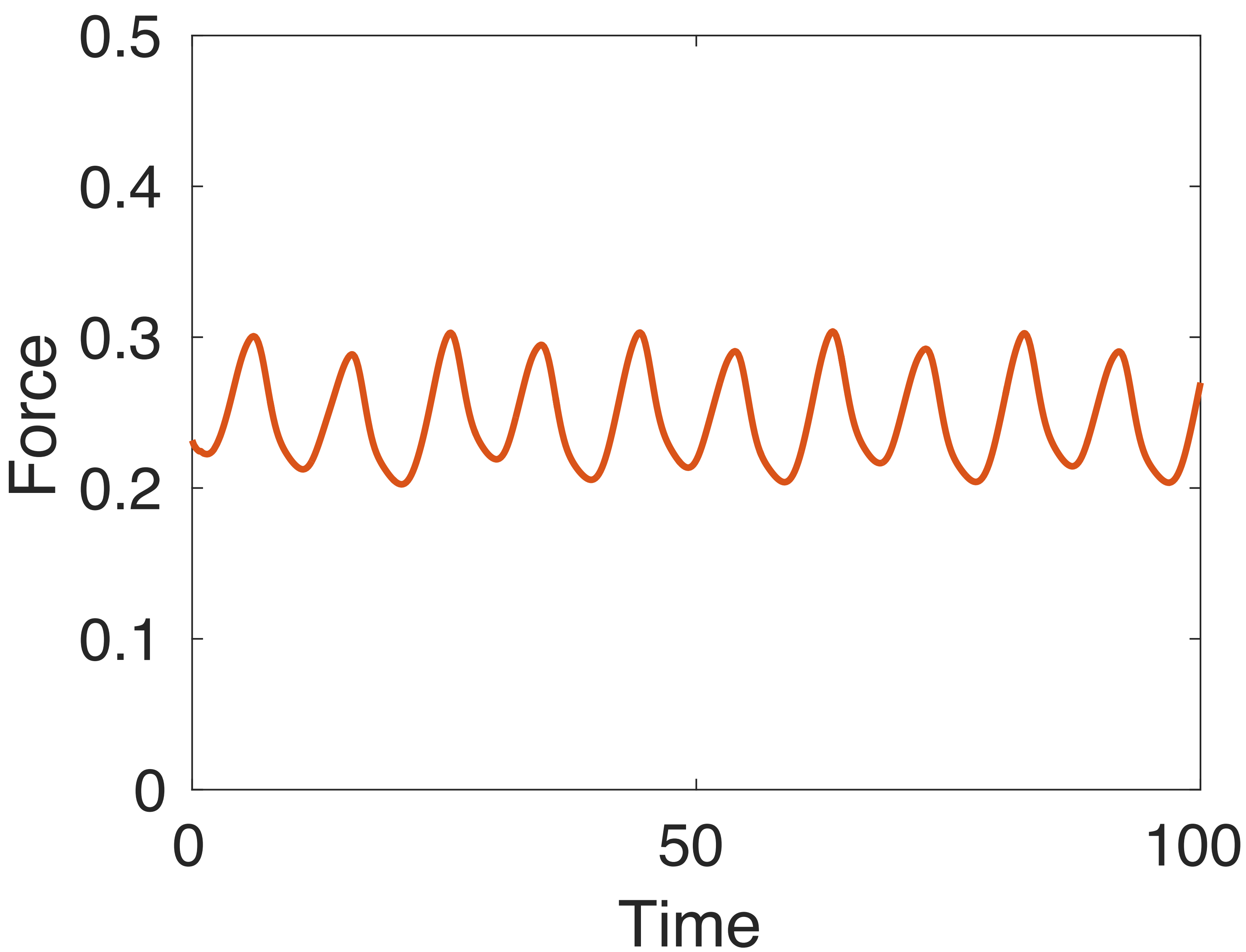

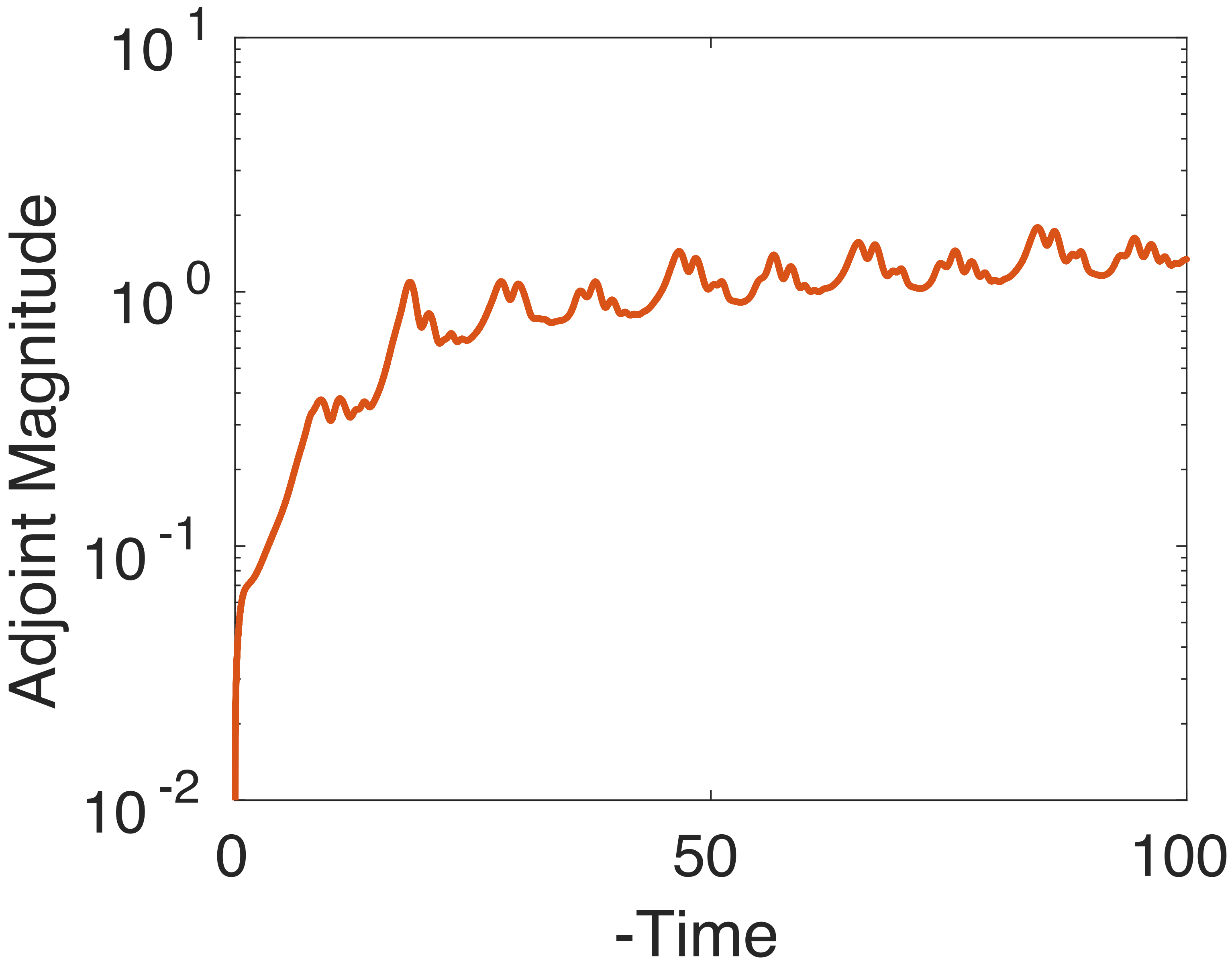

Directional Force Output

Adjoint Magnitude

- With increasing Reynolds number force has multiple frequencies
- Adjoint solution still essentially appears periodic

NACA0012, Re =2400, α = 10

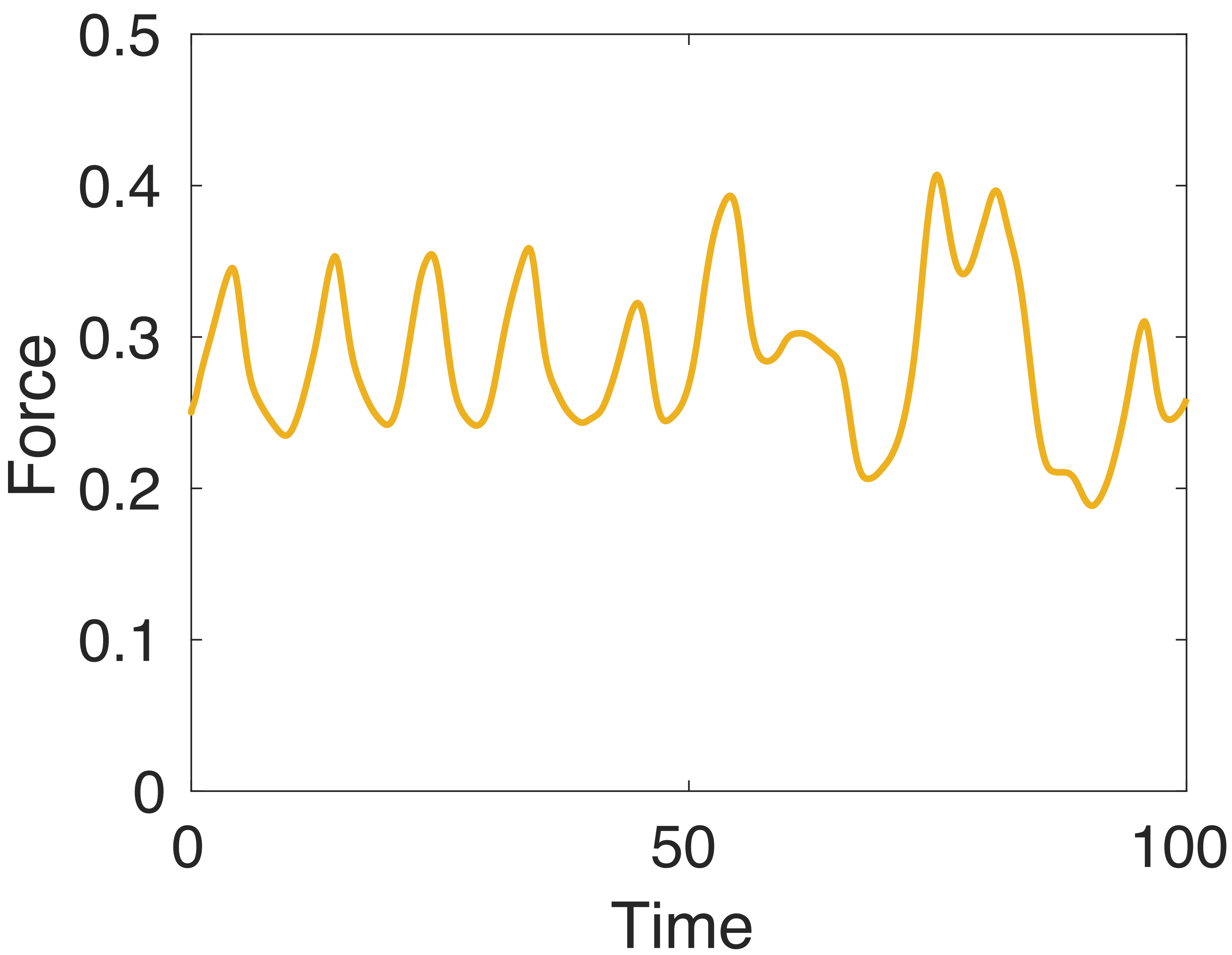

Directional Force Output

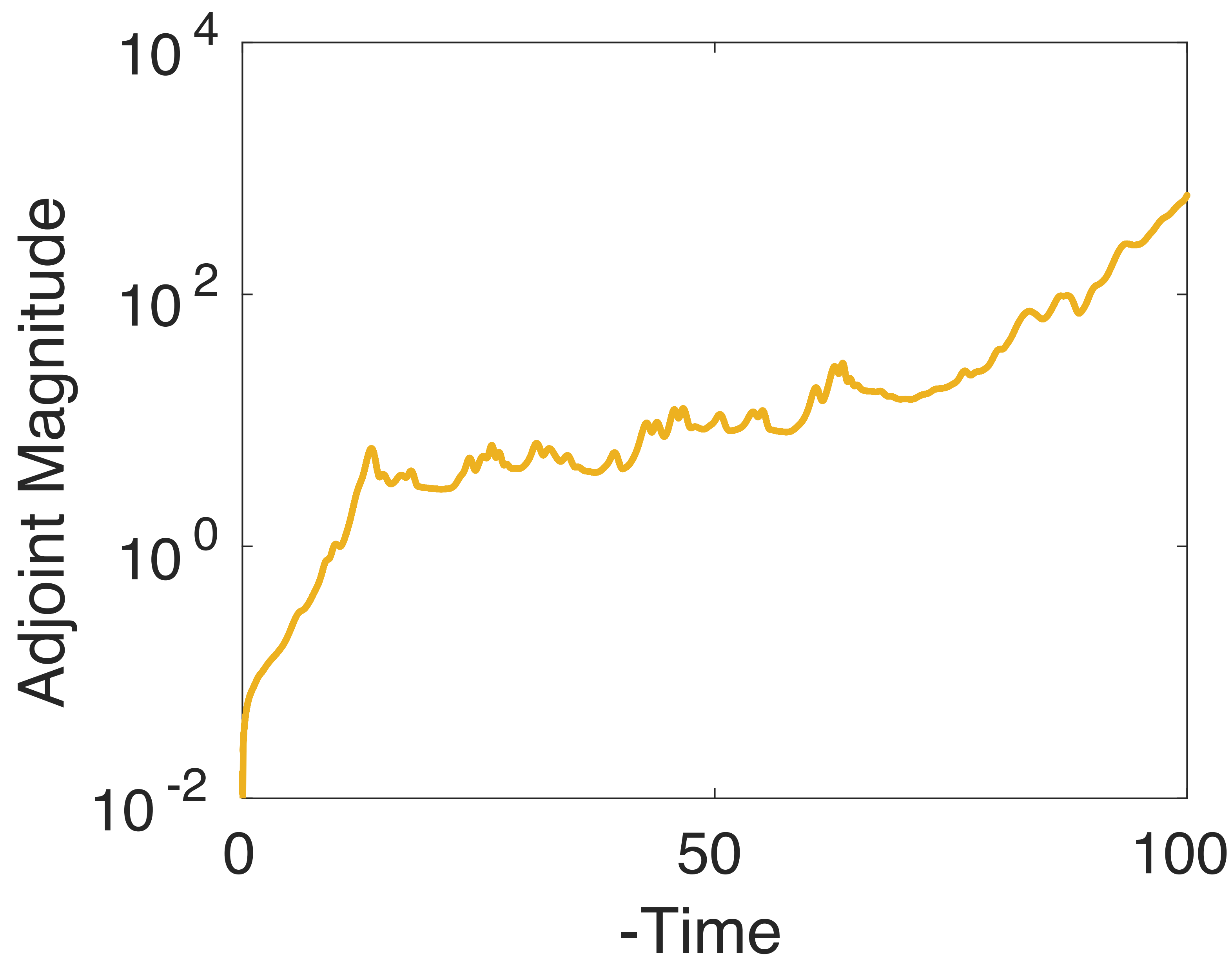

Adjoint Magnitude

- With increasing Reynolds number simulated flow become chaotic
- Adjoint solution begins to grow unboundedly

NACA0012, Re =800-2400, $\alpha = 10$

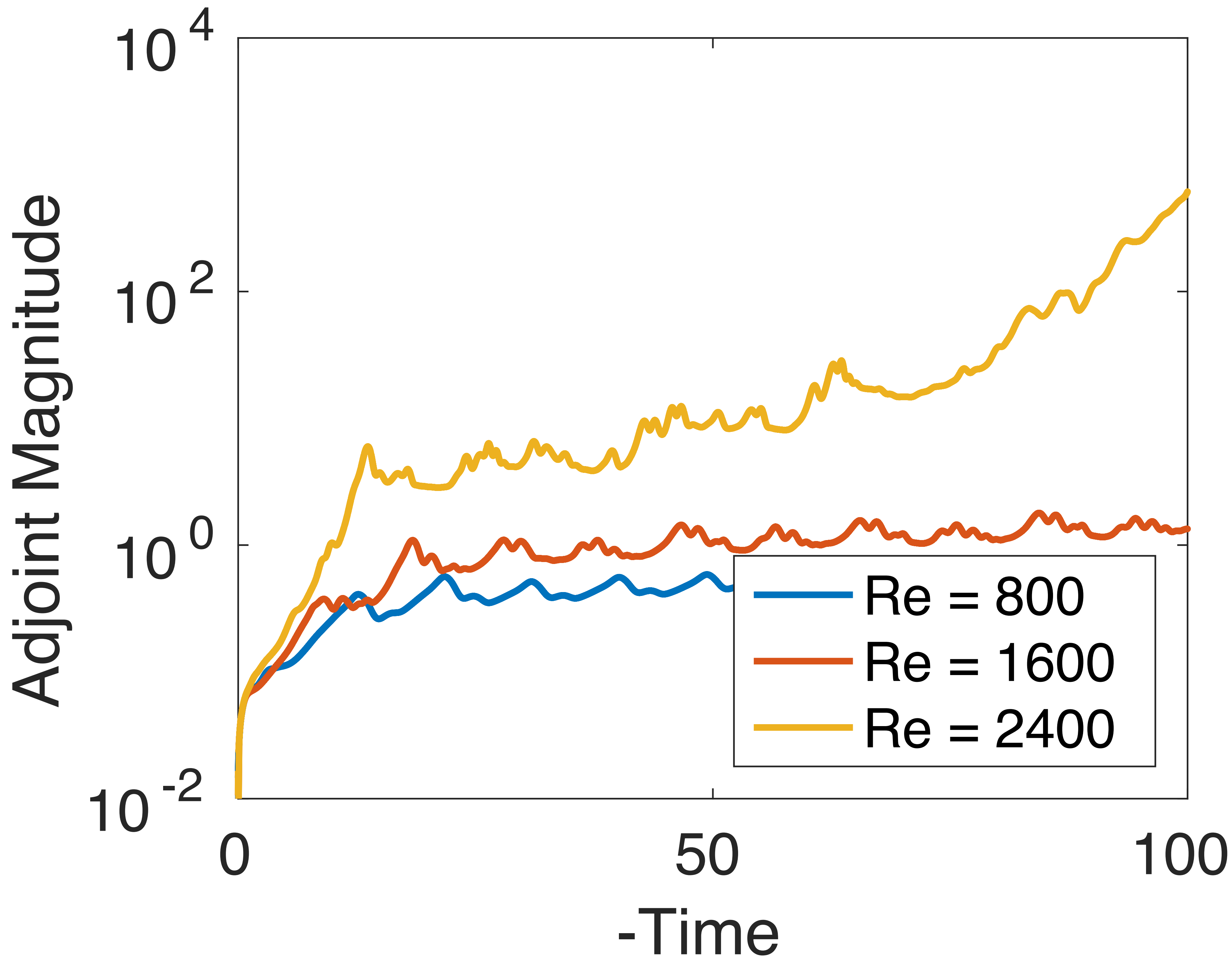

Adjoint Magnitude

- With increasing Reynolds number simulated flow become chaotic
- Adjoint solution begins to grow unboundedly

NACA0012, Re =800-2400, α = 10

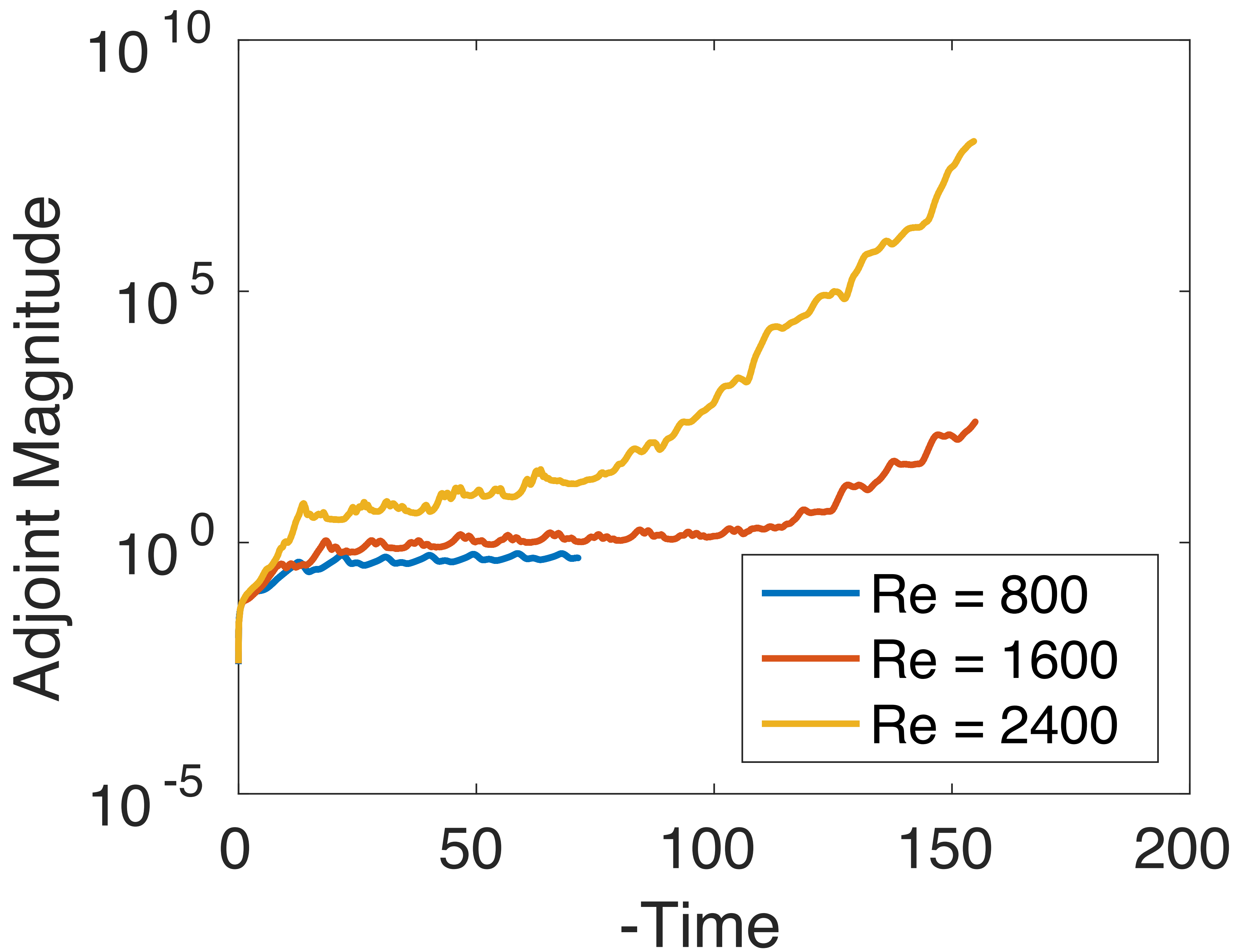

Adjoint Magnitude

- Solution is in fact chaotic at Re = 1600, but growth rate is much slower than at Re = 2400
- Windowing approaches may be successful at Re = 800, 1600

T106c Low Pressure Turbine

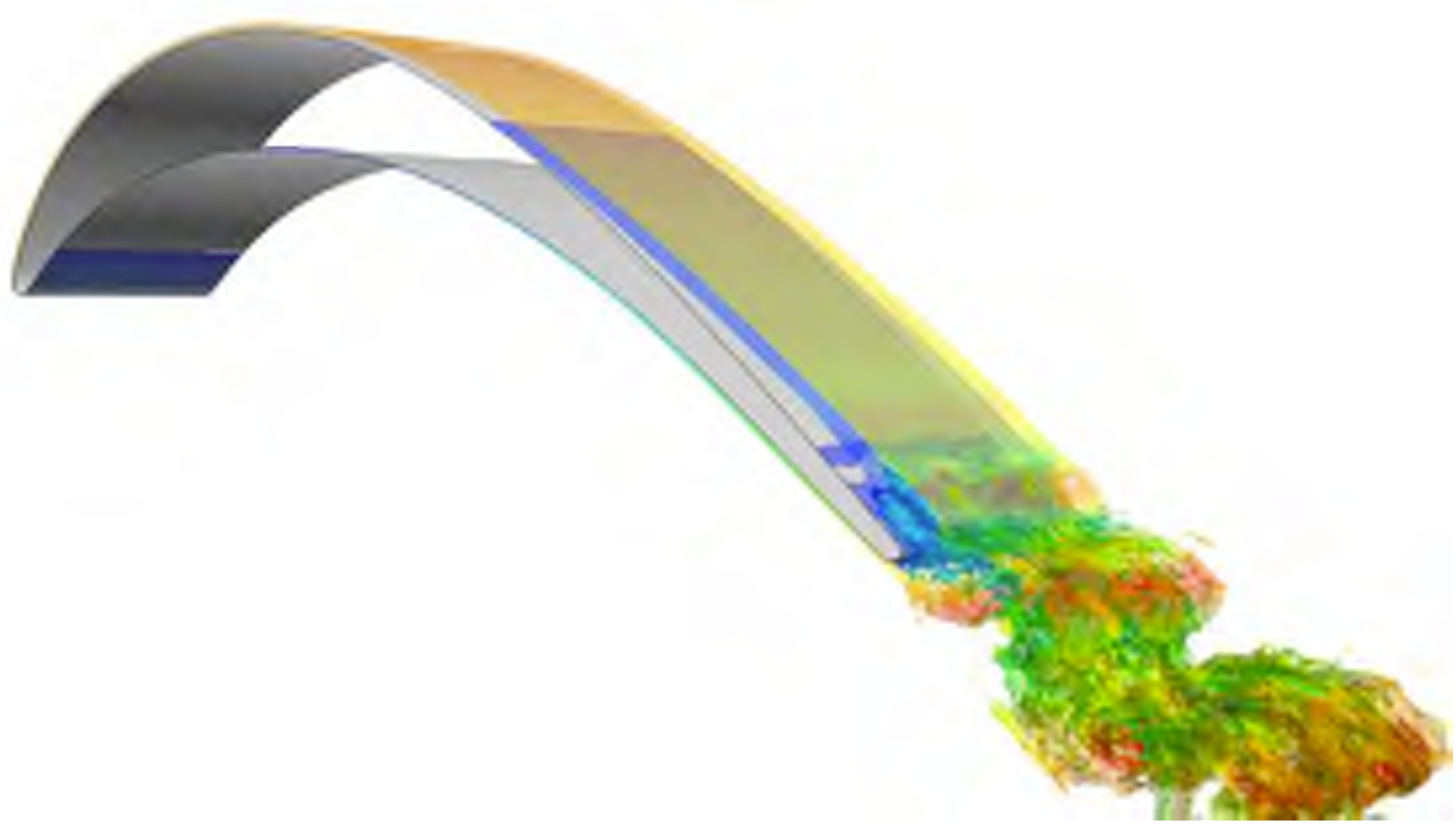

- Re = 80,000, M_{inflow} = 0.243, alpha = 32.7, M_{exit} = 0.65
- Periodic BCs in span-wise and pitch-wise directions
- No free-stream turbulence
- Spanwise domain is 20% of chord

Primal Solution

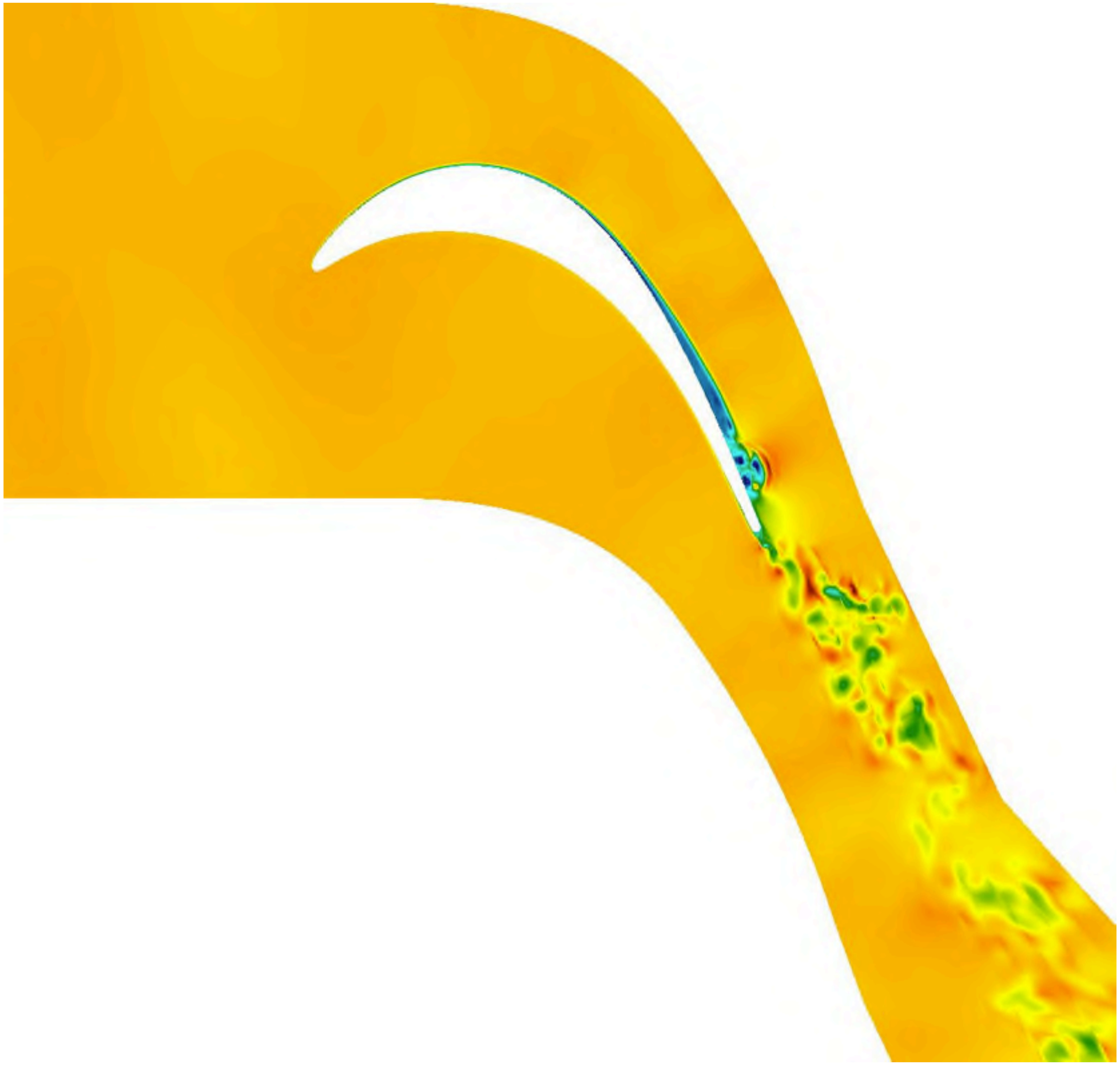

- Nearly steady flow upstream and over first 2/3 of blade
- Separation leading to transition/vortex shedding on suction-side of blade
- Fully turbulent wake

Sensitivity to Inflow Boundary Condition

- Modify inlet flow angle from α = 32.7 to α = 32.701

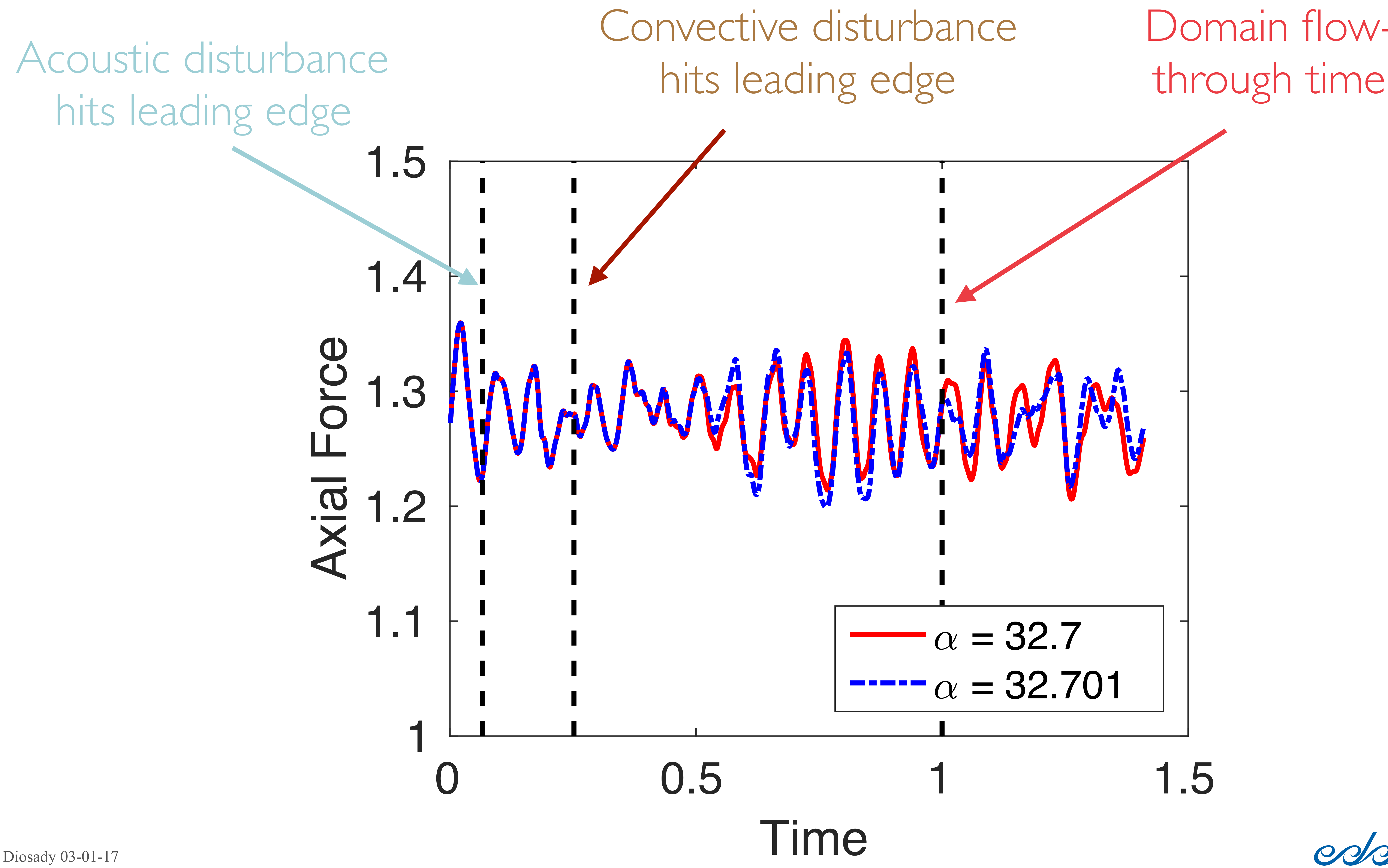

Sensitivity to Inflow Boundary Condition

Convective disturbance hits leading edge

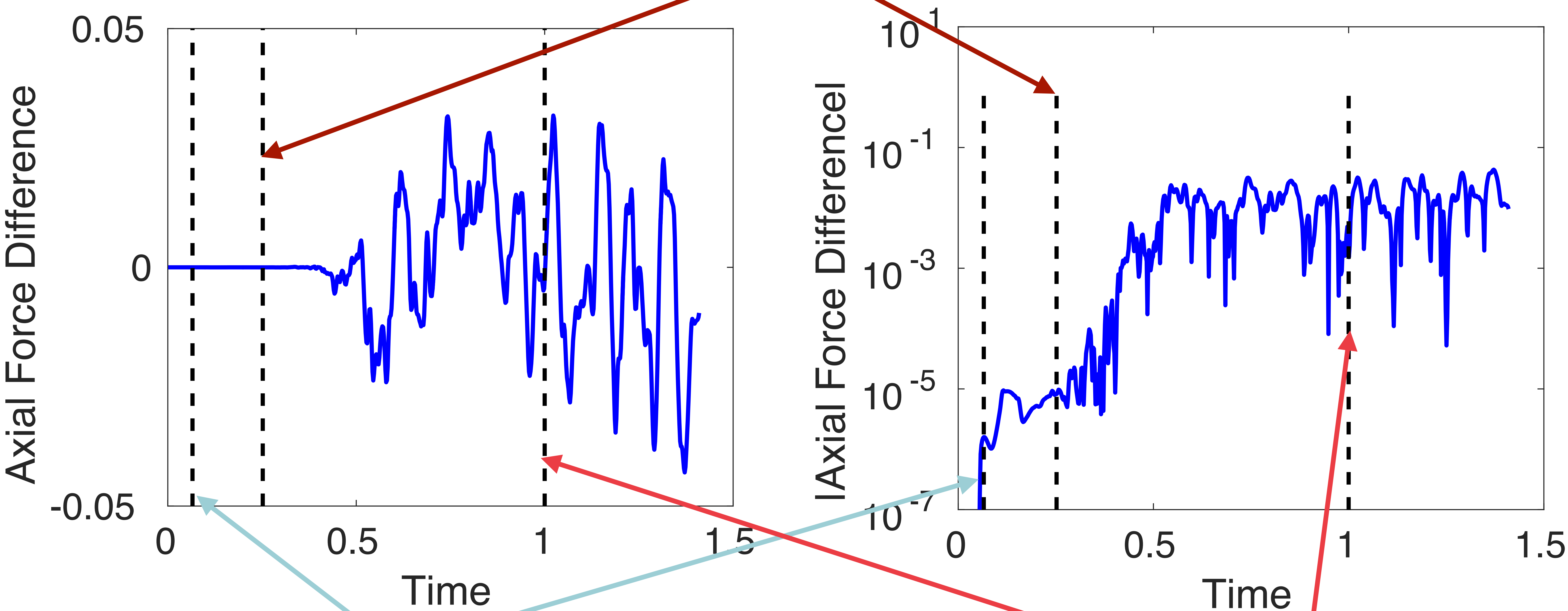

Acoustic disturbance hits leading edge

Domain flow-through time

Adjoint of mean Axial Force

- Output is integrated axial force

$$\bar{J} = \frac{1}{T}\int_0^T F_x(u(\tau))d\tau$$

- Also define output without temporal normalization

$$J(t) = \int_0^t F_x(u(\tau))d\tau$$

Sensitivity computed using adjoint

$$\Delta J(t) = J(t;\alpha+\Delta\alpha) - J(t;\alpha) = \int_0^t F_x(u(\tau;\alpha+\Delta\alpha)) - F_x(u(\tau;\alpha))d\tau$$

$$\approx \int_0^t \Psi(\tau;t,\alpha)^T R(u(\tau);\alpha+\Delta\alpha)$$

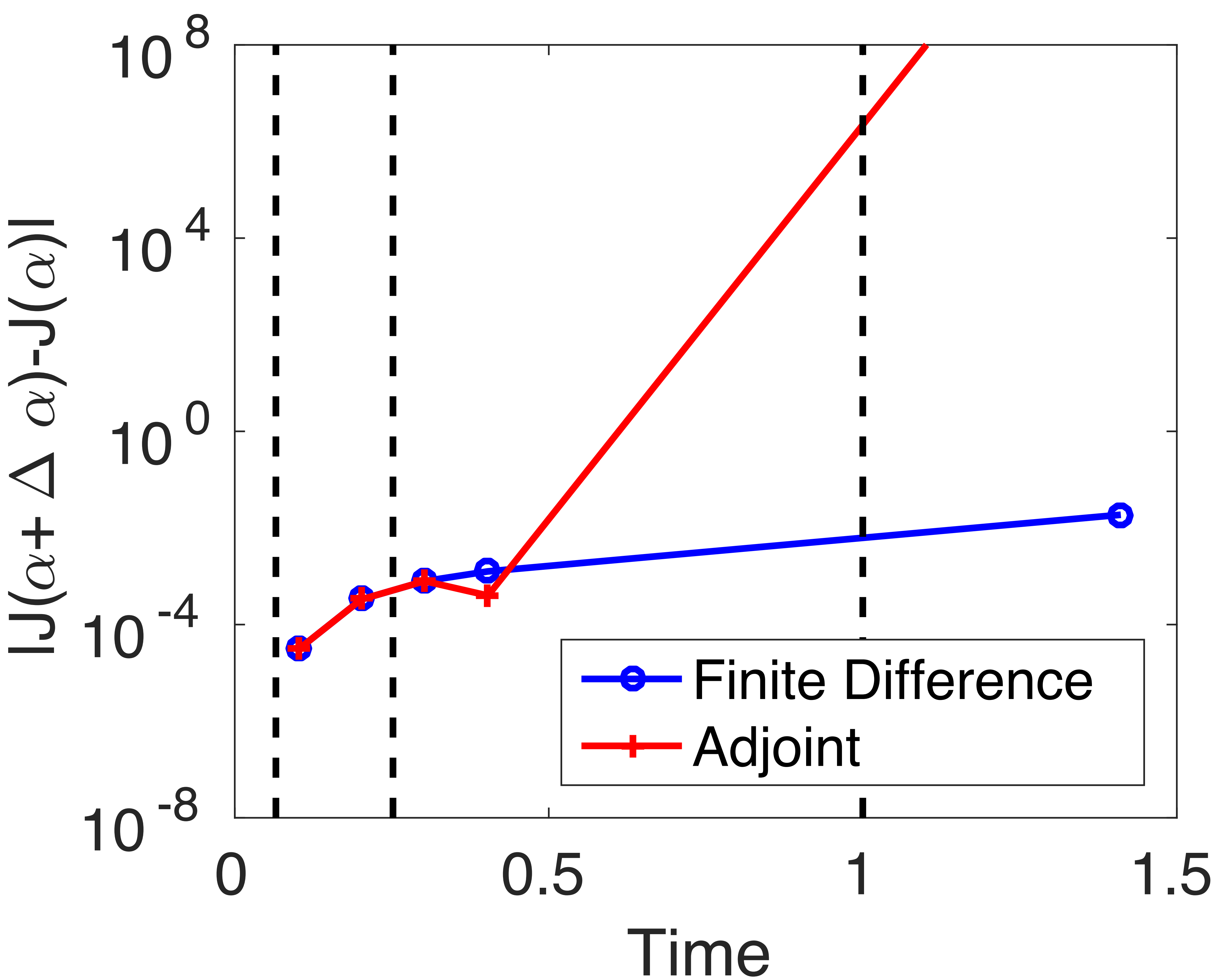

Sensitivity computed using adjoint

$$\Delta F_x(\tau) = F_x(u(\tau;\alpha+\Delta\alpha)) - F_x(u(\tau;\alpha))$$
$$?? \approx \Psi(t-\tau;t,\alpha)^T R(u;\alpha+\Delta\alpha)$$

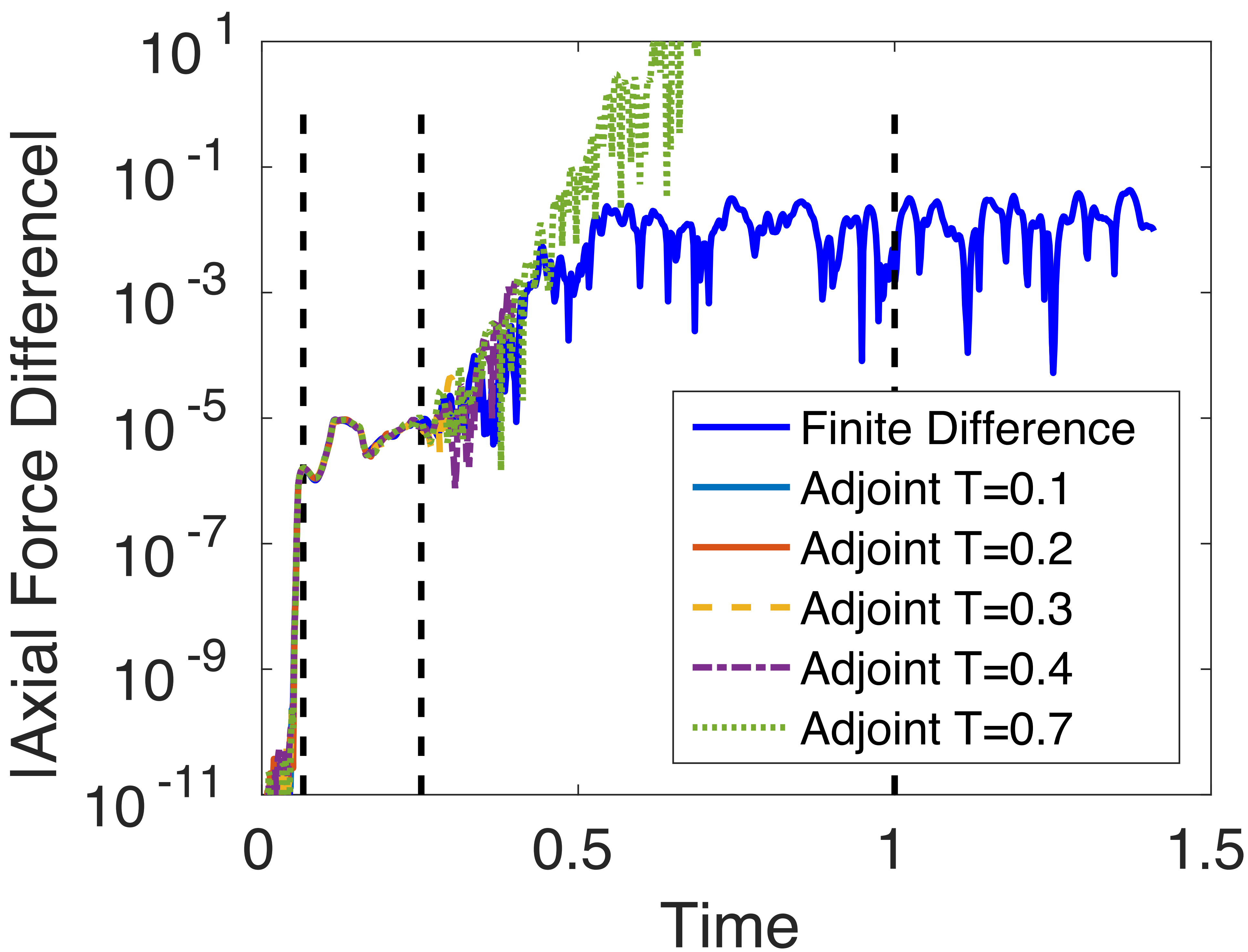

- Approximation holds since flow upstream of blade is essentially time-independent
- Adjoint correctly captures sensitivity in part of flow upstream of separation

Sensitivity computed using adjoint

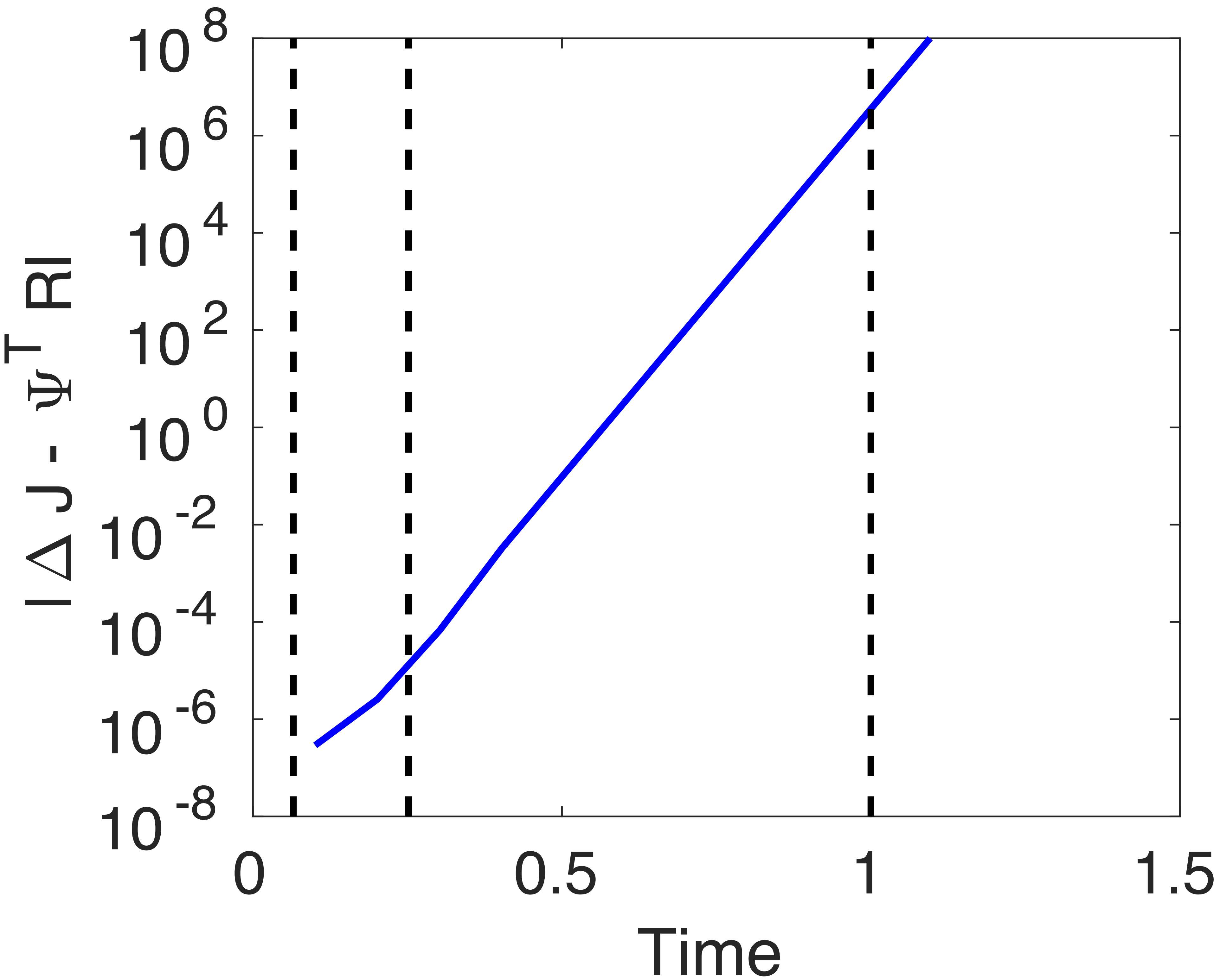

- Sensitivity computed using adjoint only valid for very short time windows
- Adjoint computed using long time window blows up
- Sensitivity computed using short time window, not representative long time behaviour

Graphical demonstration of concepts

- Adjoint correctly captures sensitivity in part of flow upstream of separation
- Sensitivity computed using adjoint only valid for very short time windows
- Sensitivity computed using short time window, not representative long time behaviour

Adjoint-based Error Estimation

- Estimate error using dual-weighted residual method (Becker & Rannacher 1995)

$$\epsilon = J(u) - J(u_H) \approx R_H(u_H, \psi_h)$$

- Localize error

$$\epsilon_\kappa \equiv R_H(u_H, \psi_h|_\kappa)$$

- Flag elements with largest error for refinement

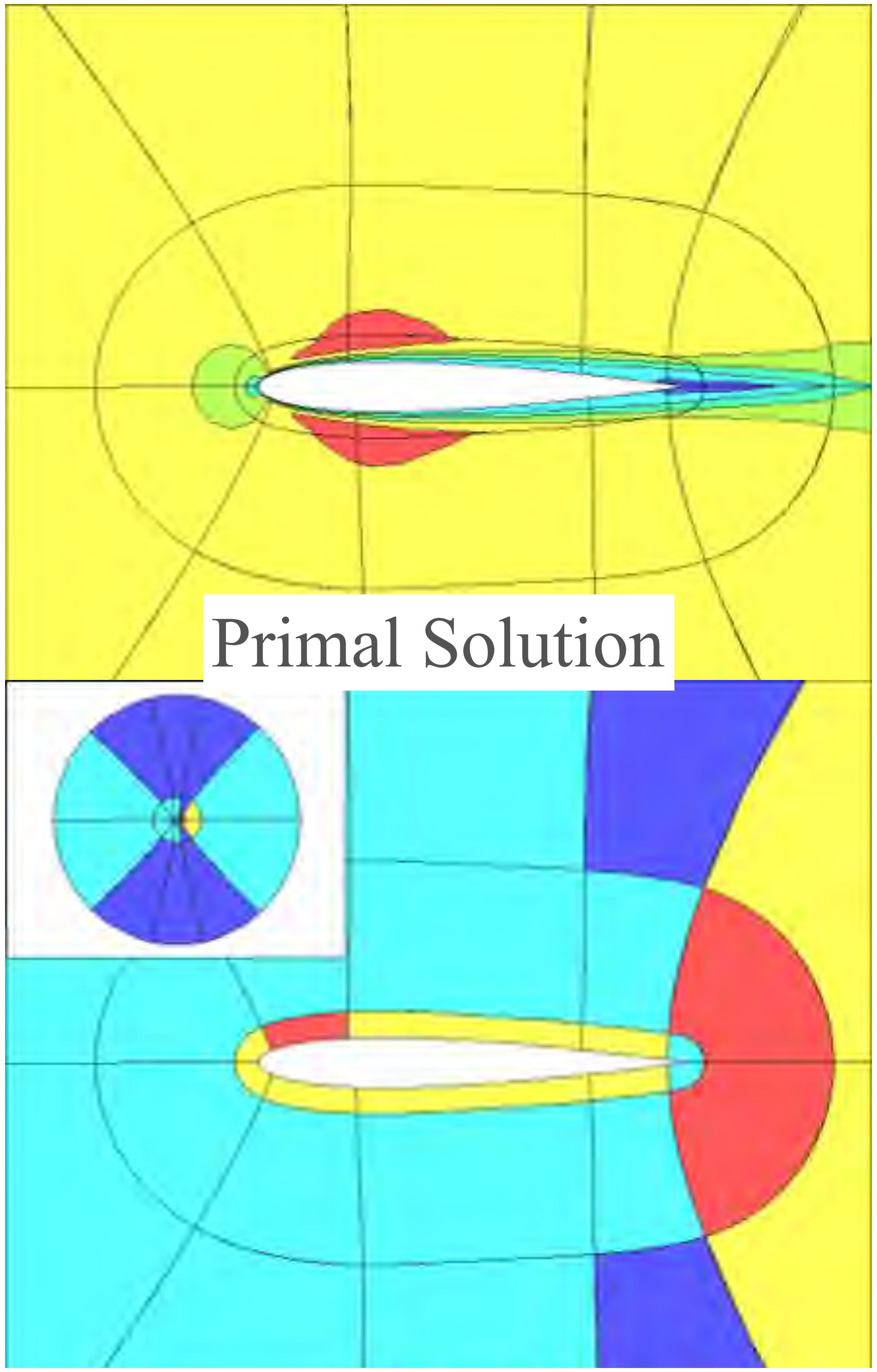

Element-based error-indicator

Adjoint-based error indicator

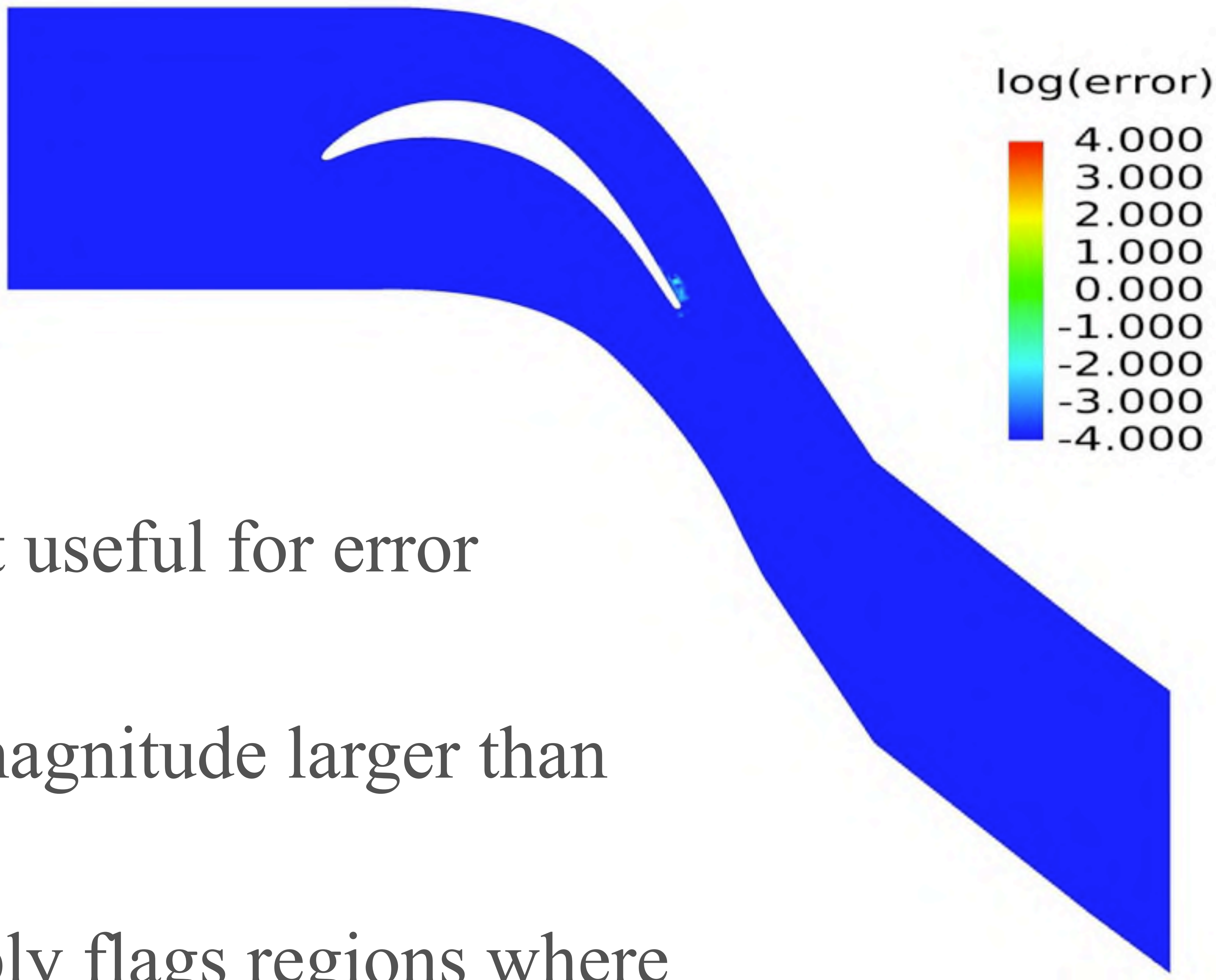

- Unbounded adjoint not useful for error estimation
- Estimate is orders of magnitude larger than actual signal
- Error localization simply flags regions where adjoint is large

Adjoint growth with mesh resolution

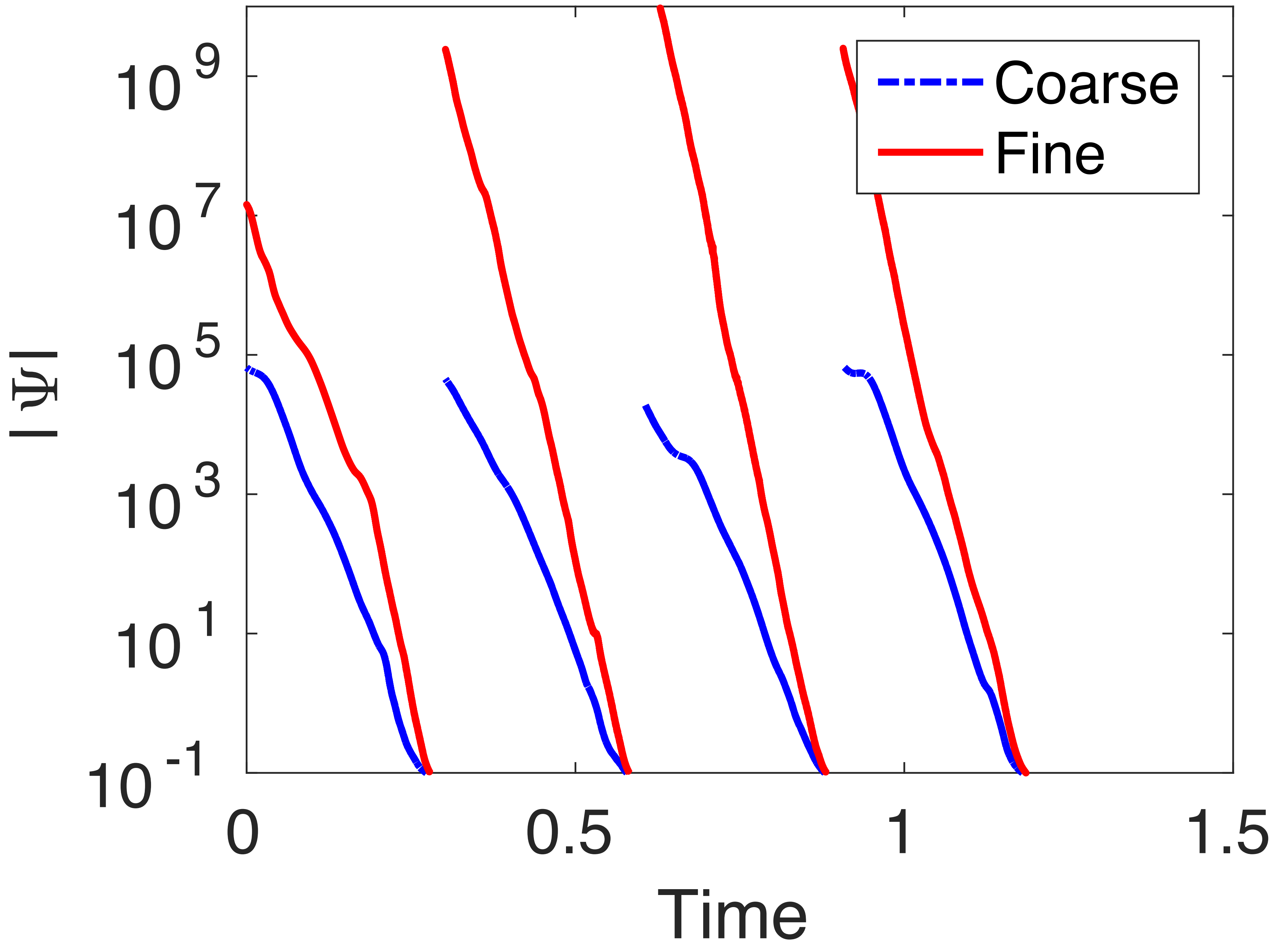

- Refined mesh has essentially double mesh resolution near separation region
- Increase mesh resolution results in faster growth of adjoint (i.e. larger Lyapunov exponent)
- Adaptation mechanism is not convergent

2

Summary

- Presented space-time adjoint solver for turbulent compressible flows
- Confirmed failure of traditional sensitivity methods for chaotic flows
- Assessed rate of exponential growth of adjoint for practical 3D turbulent simulation
- Demonstrated failure of short-window sensitivity approximations.

Questions??

Outlook/Future Work:

- Lyapunov exponents, least-square shadowing and beyond…